

Controlling escape from a potential well by reshaping periodic secondary excitations

R. Chacón¹ and J. A. Martínez²

¹*Departamento de Física Aplicada, Escuela de Ingenierías Industriales, Universidad de Extremadura, Apartado Postal 382, E-06071 Badajoz, Spain, EU*

²*Departamento de Ingeniería Eléctrica, Electrónica y Automática, Escuela Politécnica Superior, Universidad de Castilla-La Mancha, E-02071 Albacete, Spain, EU*

(Received 9 June 2009; revised manuscript received 25 October 2010; published 3 January 2011)

The role of the wave form of periodic secondary excitations at controlling (suppressing and enhancing) escape from a potential well is investigated. We demonstrate analytically (by Melnikov analysis) and numerically that a judicious choice of the excitation's wave form greatly improves the effectiveness of the escape-controlling excitations while keeping their amplitude and period fixed. These predictions are confirmed by an energy-based analysis that provides the same optimal values of the escape-controlling parameters. The example of a dissipative Helmholtz oscillator is used to illustrate the accuracy of these results.

DOI: [10.1103/PhysRevE.83.016201](https://doi.org/10.1103/PhysRevE.83.016201)

PACS number(s): 05.45.Gg, 05.45.Xt

I. INTRODUCTION

Deterministic escape from a potential well is a fundamental problem with wide-ranging implications, in which the interplay of dissipation, nonlinearity, and deterministic driving has been found to give rise to diverse escape phenomena. Examples are known in chemistry [1], quantum optics [2], astrophysics [3], and hydrodynamics [4], among many other fields, in which escape phenomena can often be well described by a low-dimensional system of differential equations. Indeed, the case that has been most extensively studied in both dissipative and Hamiltonian systems is that in which escape is induced by an escape-inducing (EI) periodic excitation added to the low-dimensional model system, so that, before escape, chaotic transients of unpredictable duration (owing to the fractal character of the basin boundary) are usually observed for orbits starting from chaotic generic phase space regions (such as those surrounding separatrices). In this scenario, the effectiveness of secondary escape-controlling (EC) periodic excitations in suppressing escape has also been demonstrated for the case of the main resonance (between the two excitations involved) in the context of dissipative systems capable of being studied by Melnikov analysis (MA) techniques [5]. This approach was further applied to the case of incommensurate EC excitations [6]. To the best of our knowledge, the overwhelming majority of studies have up to now been of the case in which both periodic excitations involved are *sinusoidal*. However, real-world excitations present a great diversity of wave forms as well as many complex transitions from one to another as the system's parameters change. This suggests studying the effectiveness of EC excitations with different wave forms at suppressing or enhancing escape while keeping their amplitudes and periods constant.

In the present work, we undertake analytical and numerical studies of this extended EC scenario by focusing on the case of the main resonance between the two excitations involved. The rest of the paper is organized as follows. Section II provides the MA-based analytical predictions for the simple model of a dissipative Helmholtz oscillator subjected to a sinusoidal EI excitation while the EC excitation is given by a periodic function with variable wave form. We also include an energy-based analysis having analytical predictions that confirm all

those from MA. Section III compares the analytical predictions of Sec. II with numerical results based on a high-resolution grid of initial conditions. Finally, Sec. IV gives a brief summary of the findings.

II. ESCAPE SUPPRESSION SCENARIO

To be specific, we shall concentrate in this paper on the simplest model for a universal escape situation: the Helmholtz oscillator [7] described by the equation

$$\ddot{x} - x + [1 + \eta \operatorname{sn}(\Omega t + \Phi; m)]x^2 = -\delta\dot{x} + \gamma \sin(\omega t), \quad (1)$$

where all variables and parameters are dimensionless. Here, $\gamma \sin(\omega t)$ and $\eta x^2 \operatorname{sn}(\Omega t + \Phi; m)$ are to be regarded as the EI and EC excitations, respectively, where $\operatorname{sn}(\cdot \cdot \cdot; m)$ is the Jacobian elliptic function of parameter $m \in [0, 1]$, $\Omega = \Omega(m, T) \equiv 4K(m)/T$, $\Phi = \Phi(m, \zeta) \equiv 2K(m)\zeta/\pi$, $\zeta \in [0, 2\pi]$, and $T \equiv 2\pi/\omega$, where $K(m)$ and T are the complete elliptic integral of the first kind and the common excitation period, respectively. When $m = 0$, one has $\operatorname{sn}(\Omega t + \Phi; m = 0) = \sin(\omega t + \zeta)$ (i.e., one recovers the canonical case of sinusoidal excitation [5]). In the other limit,

$$\operatorname{sn}(\Omega t + \Phi; m = 1) = \frac{4}{\pi} \sum_{n=1}^{\infty} \frac{\sin[(2n-1)(2\pi t/T + \zeta)]}{2n-1} \quad (2)$$

(i.e., one recovers the square-wave function of period T). The effect of renormalization of the elliptic sine argument is clear: With T constant, solely the excitation shape is varied by increasing the shape parameter m from 0 to 1, and there is thus a smooth transition from a sine function to a square wave. This allows one to study the genuine effect on the control scenario of reshaping the EC excitation.

A. Melnikov analysis

We assume that the complete system (1) satisfies the MA requirements (i.e., the dissipation and excitation terms are small-amplitude perturbations of the underlying conservative Helmholtz oscillator $\ddot{x} - x + x^2 = 0$; see Refs. [8,9] for general background information). It is worth mentioning

that the criterion for a homoclinic tangency—accurately predicted by MA—in diverse systems [4,10] is coincident with the change from a smooth to an irregular, fractal-looking basin boundary [11]. These findings connect MA predictions with those concerning the erosion of the basin boundary. A straightforward application of MA to Eq. (1) yields the Melnikov function (MF)

$$M(t_0) = -D - A \cos(\omega t_0) + \eta \sum_{n=1}^{\infty} B_n C_n \cos \left[(2n-1) \left(\frac{2\pi t_0}{T} + \zeta \right) \right],$$

$$D \equiv \frac{6\delta}{5},$$

$$A \equiv 6\pi\gamma\omega^2 \operatorname{csch}(\pi\omega), \quad (3)$$

$$B_n \equiv \frac{3}{5} \frac{\pi^2}{\sqrt{m}K(m)} \operatorname{csch} \left[(2n-1) \frac{\pi K(1-m)}{2K(m)} \right],$$

$$C_n \equiv \left[(2n-1) \frac{2\pi}{T} \right]^2 \left\{ 1 + \left[(2n-1) \frac{2\pi}{T} \right]^2 \right\} \times \left\{ 4 + \left[(2n-1) \frac{2\pi}{T} \right]^2 \right\} \operatorname{csch} \left[(2n-1) \frac{2\pi^2}{T} \right].$$

Let us assume that, in the absence of any EC excitation ($\eta = 0$), the system (1) undergoes an escape for which the respective MF

$$M_0(t_0) = -D - A \cos(\omega t_0) \quad (4)$$

has simple zeros (i.e., $D \leq A$), where the equals sign corresponds to the case of tangency between the stable and unstable manifolds [9]. If we now let the EC excitation act on the system such that $B^* \leq A - D$, with

$$B^* \equiv \max_{t_0} \left\{ \eta \sum_{n=1}^{\infty} B_n C_n \cos \left[(2n-1) \left(\frac{2\pi t_0}{T} + \zeta \right) \right] \right\}, \quad (5)$$

this relationship represents a sufficient condition for $M(t_0)$ to change sign at some t_0 . Thus, a necessary condition for $M(t_0)$ always to have the same sign is

$$B^* > A - D \equiv B_{\min}. \quad (6)$$

Since $B_n > 0, C_n > 0, n=1, 2, \dots$, one has $B^* \leq \eta \sum_{n=1}^{\infty} B_n C_n$ (see the Appendix) and hence

$$\eta > \eta_{\min} \equiv \left(1 - \frac{D}{A} \right) R, \quad (7)$$

$$R_s = R(\gamma, T, m) \equiv \frac{A}{\sum_{n=1}^{\infty} B_n C_n}.$$

Equation (7) provides a lower threshold for the amplitude of the EC excitation. Similarly, an upper threshold is obtained by imposing the condition that the EC excitation may not enhance the initial escape; that is,

$$B^* \leq \eta \sum_{n=1}^{\infty} B_n C_n < A + D \equiv B_{\max}, \quad (8)$$

and hence

$$\eta < \eta_{\max} \equiv \left(1 + \frac{D}{A} \right) R, \quad (9)$$

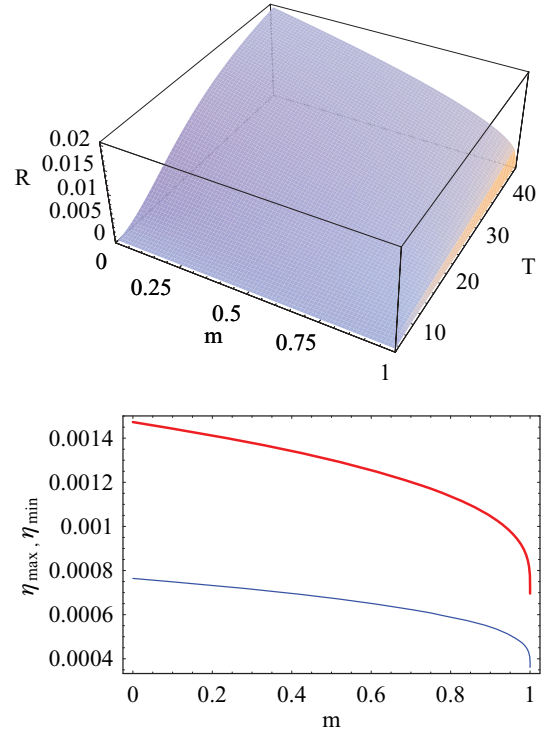


FIG. 1. (Color online) Top: Surface plot of the function R [cf. Eqs. (7) and (3)] vs shape parameter m and period T . Bottom: Threshold amplitudes η_{\min} and η_{\max} [Eqs. (7) and (9), respectively] vs shape parameter m for $T = 2\pi/0.85$. System parameters: $\gamma = 0.1$ and $\delta = 0.05$. The quantities plotted are dimensionless.

which is a necessary condition for $M(t_0)$ always to have the same sign. Thus, the suitable (suppressive) amplitudes of the EC excitation must satisfy

$$\eta_{\min} < \eta < \eta_{\max}. \quad (10)$$

Figure 1 shows how both the threshold amplitudes $\eta_{\min, \max}$ and the width of the range of suitable amplitudes $\Delta\eta \equiv \eta_{\max} - \eta_{\min} = 2(D/A)R$ decrease as the shape parameter m is increased from 0 to 1 due to the dependence of the function R on the shape parameter. In other words, ever lower amplitudes η_{\min} can suppress escape as the EC excitation wave form approaches a square wave, while the corresponding suppressory ranges $\Delta\eta$ also decrease, owing to the enhancement of the escape-inducing effectiveness of the EC excitation.

Regarding suitable values of the initial phase difference ζ , note that ζ determines the relative phase between $M_0(t_0)$ and $\eta \sum_{n=1}^{\infty} B_n C_n \cos[(2n-1)(\frac{2\pi t_0}{T} + \zeta)]$ irrespective of the shape parameter value. We therefore conclude from previous theory [12] that a sufficient condition for $\eta_{\min} < \eta < \eta_{\max}$ also to be a sufficient condition for suppressing escape is that $M_0(t_0)$ and $\eta_{\min, \max} \sum_{n=1}^{\infty} B_n C_n \cos[(2n-1)(\frac{2\pi t_0}{T} + \zeta)]$ are in opposition. This yields the optimal suppressory value

$$\zeta_{\text{opt}}^{\text{sup}} = 0 \quad (11)$$

for all $m \in [0, 1]$, in the sense that they allow the widest amplitude ranges for the EC excitation. Similarly, we see that imposing $M_0(t_0)$ to be in phase with $\eta_{\min, \max} \sum_{n=1}^{\infty} B_n C_n \cos[(2n-1)(\frac{2\pi t_0}{T} + \zeta)]$ is a sufficient condition for $M(t_0)$ to change

sign at some t_0 . This condition provides the optimal enhancer values of the initial phase difference

$$\zeta_{\text{opt}}^{\text{enh}} = \pi, \quad (12)$$

in the sense that $M(t_0)$ presents its highest maximum at $\zeta_{\text{opt}}^{\text{enh}}$ (i.e., one obtains the maximum gap from the homoclinic tangency condition).

B. Energy-based analysis

An alternative physical explanation of the foregoing MA-based predictions results from analyzing the variation of the system's energy. Indeed, Eq. (1) has the associated energy equation

$$\frac{dE}{dt} = -\delta\dot{x}^2 + \gamma\dot{x} \sin(\omega t) - \eta\dot{x}x^2 \text{sn}(\Omega t + \Phi; m), \quad (13)$$

where $E(t) \equiv (1/2)\dot{x}^2(t) + U[x(t)]$ [$U(x) \equiv -x^2/2 + x^3/3$] is the energy function. Integration of Eq. (13) over any interval $[nT, nT + T/2]$, $n = 0, 1, 2, \dots$, yields

$$\begin{aligned} E(nT + T/2) &= E(nT) - \delta \int_{nT}^{nT+T/2} \dot{x}^2(t) dt \\ &\quad - \eta \int_{nT}^{nT+T/2} \dot{x}(t)x^2(t) \text{sn}(\Omega t + \Phi; m) dt \\ &\quad + \gamma \int_{nT}^{nT+T/2} \dot{x}(t) \sin(\omega t) dt. \end{aligned} \quad (14)$$

Now, if we consider fixing the parameters (δ, γ, T) for the system to undergo an escape at $\eta = 0$, there always exists an $n = n^*$ such that the energy increment $\Delta E \equiv E(n^*T + T/2) - E(n^*T)$ is positive just before escape. Thus, after applying the first Mean Value Theorem [13], together with well-known properties of the Jacobian elliptic functions [14], to the last two integrals on the right-hand side of Eq. (14),

$$\begin{aligned} E(n^*T + T/2) &= E(n^*T) - \delta \int_{n^*T}^{n^*T+T/2} \dot{x}^2(t) dt + \frac{\gamma T}{\pi} \dot{x}(t^*) \\ &\quad - \frac{\eta \dot{x}(t^{**})x^2(t^{**})}{4} F(\zeta, m), \end{aligned} \quad (15)$$

where $t^*, t^{**} \in [n^*T, n^*T + T/2]$ and

$$F(\zeta, m) \equiv \frac{1}{\sqrt{m}K(m)} \ln \left(\frac{1 + \sqrt{m} \text{cd}[2K(m)\zeta/\pi]}{1 - \sqrt{m} \text{cd}[2K(m)\zeta/\pi]} \right), \quad (16)$$

where $\text{cd}(\dots; m) \equiv \text{cn}(\dots; m)/\text{dn}(\dots; m)$, one has $\gamma T \dot{x}(t^*)/\pi > \delta \int_{n^*T}^{n^*T+T/2} \dot{x}^2(t) dt$ at $\eta = 0$ just before escape. It is straightforward to see that $F(\zeta, m)$ is a 2π -periodic function in ζ and presents the noteworthy properties (see Fig. 2)

$$\begin{aligned} F(\pi, m) &= -F(0, m) = \frac{\ln[(1 - \sqrt{m})/(1 + \sqrt{m})]}{\sqrt{m}K(m)}, \\ F(\pi/2, m) &= F(3\pi/2, m) = 0, \\ \lim_{m \rightarrow 1} F(0, m) &= -\lim_{m \rightarrow 1} F(\pi, m) = 2, \\ \lim_{m \rightarrow 0} F(0, m) &= -\lim_{m \rightarrow 0} F(\pi, m) = \frac{4}{\pi}. \end{aligned} \quad (17)$$

In this situation, one lets the EC excitation act on the system while holding the remaining parameters constant.

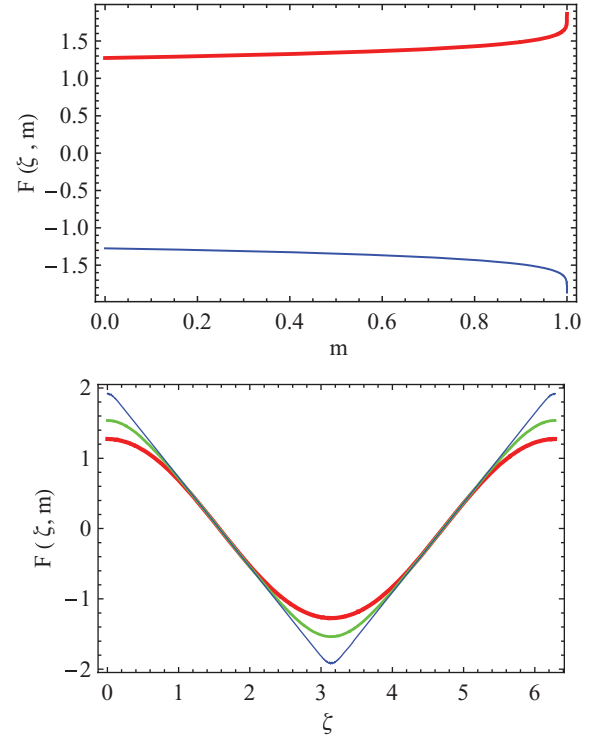


FIG. 2. (Color online) Plots of the function $F(\zeta, m)$ [see Eq. (16)]. Top panel: F vs m for $\zeta = 0$ (thick line) and π (thin line). Bottom panel: F vs ζ for $m = 0$ (thick line), 0.95 (medium line), and $1 - 10^{-14}$ (thin line). The quantities plotted are dimensionless.

For sufficiently small values of $\eta > 0$, one expects that both the dissipation work [integral in Eq.(15)] and $\dot{x}(t^*)$ will approximately maintain their initial values (at $\eta = 0$) while the function $F(\zeta, m)$ will increase (decrease) from 0 (at $\zeta = \pi/2$ and $3\pi/2$), so that, in some cases depending upon the remaining parameters (see Fig. 2), the energy increment just before escape ΔE could be sufficiently large and negative (positive) to suppress (enhance) the initial escape. Clearly, the probability of suppressing (enhancing) the initial escape is maximal at $m = 1$ and $\zeta = 0$ ($\zeta = \pi$), which is in complete agreement with the foregoing MA-based predictions.

III. INHIBITION OF THE EROSION OF NON ESCAPING BASINS

For the universal escape model (1), the initial conditions will determine, for a fixed set of its parameters, whether the system escapes to an attractor at infinity (with $x \rightarrow -\infty$ as $t \rightarrow \infty$), or settles into a bounded oscillation. In a series of papers, Thompson and co-workers [4,15,16] have shown for the system

$$\ddot{x} + x - x^2 = -\delta\dot{x} + \gamma \sin(\omega t) \quad (18)$$

that there can exist a dramatic and rapid erosion of the safe basin (union of the basins of the bounded attractors) due to encroachment by the basin of the attractor at infinity (escaping basin). Since the same escape scenario occurs for the closely related system (1) in the absence of an escape-suppressing

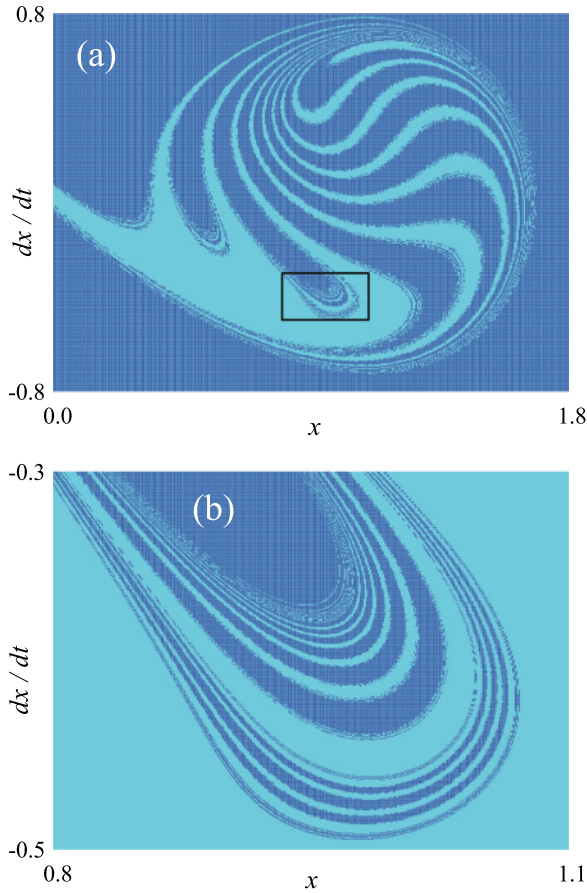


FIG. 3. (Color online) Basin erosion of the system (1) with $\eta = 0$ (a) in the window $0 \leq x \leq 1.8, -0.8 \leq \dot{x} \leq 0.8$, and (b) detail corresponding to the window $0.8 \leq x \leq 1.1, -0.5 \leq \dot{x} \leq -0.3$ [rectangle in version (a)]. The color cyan (pale gray) represents the nonescaping basin and blue (black) represents the escaping basin. System parameters: $\gamma = 0.08, \delta = 0.1$, and $T = 2\pi/0.85$. The quantities plotted are dimensionless.

(ES) excitation ($\eta = 0$), we shall show in the following how the safe basin is restored when $\eta > 0$, according to the MA and energy-based analysis predictions. The basins of attraction were computed by using a fourth-order Runge-Kutta algorithm with time steps in the range $\Delta t = 0.005-0.01$. To generate numerically the basins of attraction, we selected a grid of 400×400 uniformly distributed starting points in the region of phase space $\{x(t=0) \in [0, 1.8], \dot{x}(t=0) \in [-0.8, 1]\}$. From this grid of initial conditions, each integration is continued until either x exceeds 20, at which point the system is deemed to have escaped (i.e., to the attractor at infinity), or the maximum allowable number of cycles, here 20, is reached. The color cyan (pale gray) represents the nonescaping basin and blue (black) represents the escaping basin. In the absence of an EC excitation ($\eta = 0$), we assume that the system presents a dramatic erosion and stratification of the basin (as in the example shown in Fig. 3).

Figure 4 shows the lowest value of the EC amplitude η'_{\min} , for which the erosion of the safe basin has completely disappeared, as a function of the shape parameter m (dots). One sees that η'_{\min} decreases as the EC excitation wave form approaches a square wave, and that the experimental points fit

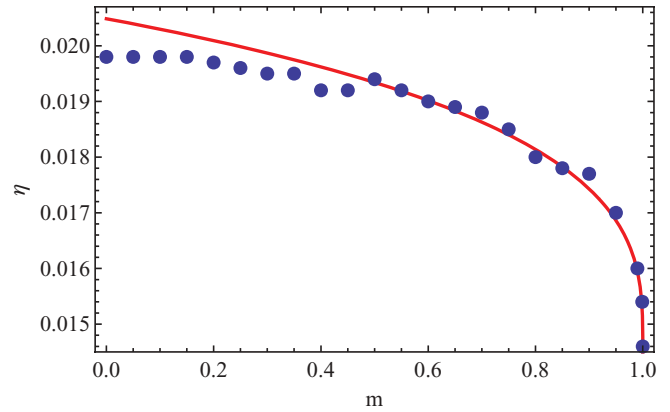


FIG. 4. (Color online) Lowest value of the EC amplitude η preserving the safe basin without erosion (dots, see the text) and lower threshold for suppression of chaotic escape η_{\min} [solid line, Eq. (7)] vs shape parameter m . System parameters: $\gamma = 0.08, \delta = 0.1$, and $T = 2\pi/0.85$. The quantities plotted are dimensionless.

the analytical estimate η_{\min} [solid line, Eq. (7)]. This decrease is especially fast for values of m very close to 1, which is a consequence of the dependence of $K(m)$ on m [17].

As mentioned in the preceding section, the initial phase difference ζ plays a fundamental role in the suppression or enhancement of escape, irrespective of the shape parameter value. To test the predictions concerning the dependence of the escape scenario on ζ , we calculated the escape probability normalized to that of the corresponding case with no EC excitation, $P(\eta > 0)/P(\eta = 0)$, vs ζ for several values of m . Figure 5 shows an illustrative example comparing the cases corresponding to $m = 0$ (sinusoidal wave form), $m = 1-10^{-14}$ (square wave form), and $m = 0.95$ (an intermediate wave form), in which the numerical results confirm the theoretical predictions of Sec. II. Specifically, one finds in general that a square wave has a greater effectiveness at controlling escape than a sinusoidal wave form, as predicted. However,

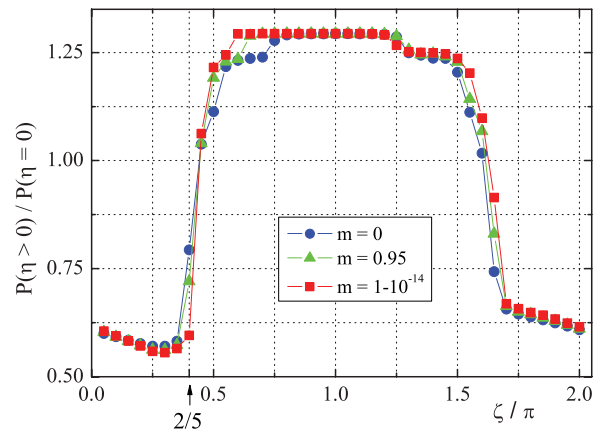


FIG. 5. (Color online) Normalized escape probability (see the text) vs initial phase difference for three values of the shape parameter: $m = 0$ (circles), $m = 0.95$ (triangles), and $m = 1-10^{-14}$ (squares). System parameters: $\eta = 0.05, \gamma = 0.08, \delta = 0.1$, and $T = 2\pi/0.85$. Straight lines are plotted solely to guide the eye. The quantities plotted are dimensionless.

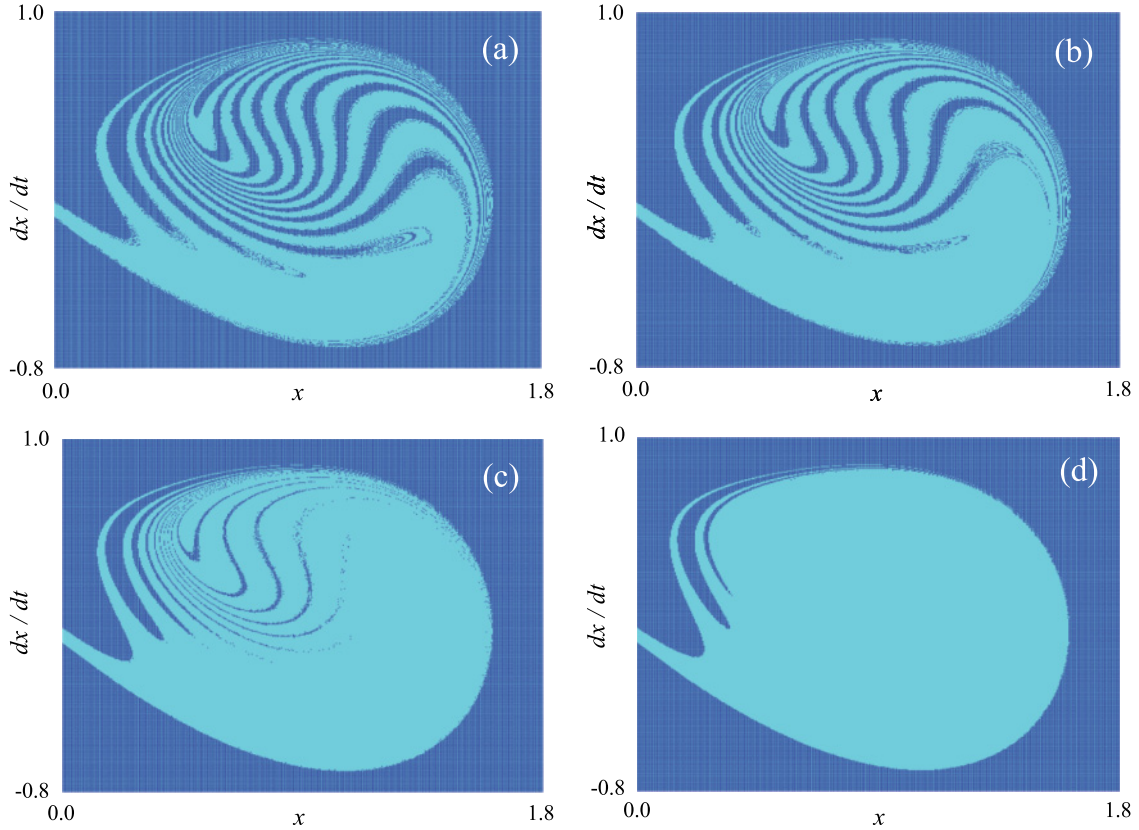


FIG. 6. (Color online) Restoration of the safe basin of the system (1) in the window $0 \leq x \leq 1.8, -0.8 \leq \dot{x} \leq 1$ for $\eta = 0.05$, $\gamma = 0.08$, $\delta = 0.1$, $T = 2\pi/0.85$, and $\zeta = 2\pi/5$, and four values of the shape parameter: (a) $m = 0$, (b) $m = 0.9$, (c) $m = 0.999$, and (d) $m = 1 - 10^{-14}$. The color cyan (pale gray) represents the nonescaping basin and blue (black) represents the escaping basin.

such a greater effectiveness is hardly noticeable at the optimal suppressory and enhancer values of the initial phase difference, $\zeta_{\text{opt}}^{\text{sup}} = 0$ and $\zeta_{\text{opt}}^{\text{enh}} = \pi$ (see Fig. 5). Remarkably, the escape scenario is very sensitive to reshaping of the EC excitation over certain ranges of the initial phase difference around the values $\zeta = \pi/2$ and $3\pi/2$, respectively (i.e., those values of the initial phase difference having neither a significant suppressor effect nor a significant enhancer effect; cf. Sec. III). An illustrative example is shown in Fig. 6 for the value $\zeta = 2\pi/5$ (see Fig. 5) and four values of the shape parameter $m = 0, 0.9, 0.999$, and $1 - 10^{-14}$. One sees a gradual (but incomplete) basin restoration sequence as a sinusoidal EC excitation [$m = 0$, Fig. 6(a)] transforms into a square-wave EC excitation [$m = 1 - 10^{-14}$, Fig. 6(d)]. It is worth mentioning that the present reshaping-induced modification of a fractal basin boundary from having fractal-like fingers protruding into the nonescaping basin [as in Figs. 6(a), 6(b), and 6(c)] to their almost complete disappearance [as in Fig. 6(d)] has previously been observed in a driven dissipative oscillator with a cubic potential that typically models a metastable system close to a fold [18].

IV. CONCLUDING REMARKS

To conclude, we have demonstrated that judiciously tailoring the wave form of periodic secondary excitations greatly improves their effectiveness in controlling (suppressing and

enhancing) the escape from a potential well that is induced by primary periodic excitations. Numerical results, based on a high-resolution grid of initial conditions, showed good agreement with theoretical predictions obtained from two independent approaches: Melnikov analysis and energy-based analysis. The present findings can be readily tested experimentally (for instance, in electronic and laser systems [19–21]), and can find application for improving the control of elementary dynamic processes characterized by escape from a potential well, such as transport phenomena in dissipative lattices as well as diverse atomic and molecular processes.

ACKNOWLEDGMENTS

R.Ch. acknowledges partial financial support from the Ministerio de Ciencia e Innovación (MCI, Spain) through Project No. FIS2008-01383.

APPENDIX: DERIVATION OF THE FORMULA

$$B^* \leq \eta \sum_{n=1}^{\infty} B_n C_n$$

Using the formula [15]

$$\cos(px) = \cos(x) \prod_{k=1}^{(p-1)/2} \left\{ 1 - \frac{\sin^2 x}{\sin^2 \left[\frac{(2k-1)\pi}{2p} \right]} \right\}, \quad p \text{ odd}, \quad (\text{A1})$$

one has

$$\begin{aligned} & \left| \sum_{n=1}^{\infty} B_n C_n \cos \left[(2n-1) \left(\frac{2\pi t_0}{T} + \zeta \right) \right] \right| \\ &= \left| \sum_{n=1}^{\infty} B_n C_n \prod_{k=1}^{n-1} \left\{ 1 - \frac{\sin^2 \left(\frac{2\pi t_0}{T} + \zeta \right)}{\sin^2 \left[\frac{(2k-1)\pi}{4n-2} \right]} \right\} \cos \left(\frac{2\pi t_0}{T} + \zeta \right) \right| \\ &\leq \left| \sum_{n=1}^{\infty} B_n C_n \cos \left(\frac{2\pi t_0}{T} + \zeta \right) \right|, \end{aligned} \quad (\text{A2})$$

and hence

$$\begin{aligned} B^* &\equiv \max_{t_0} \left\{ \eta \sum_{n=1}^{\infty} B_n C_n \cos \left[(2n-1) \left(\frac{2\pi t_0}{T} + \zeta \right) \right] \right\} \\ &\leq \max_{t_0} \left\{ \eta \sum_{n=1}^{\infty} B_n C_n \cos \left(\frac{2\pi t_0}{T} + \zeta \right) \right\} \\ &\leq \eta \sum_{n=1}^{\infty} B_n C_n. \end{aligned} \quad (\text{A3})$$

-
- [1] M. E. Goggin and P. W. Milonni, *Phys. Rev. A* **37**, 796 (1988).
- [2] R. Chacón and J. I. Cirac, *Phys. Rev. A* **51**, 4900 (1995).
- [3] G. Contopoulos, H. Handrup, and D. Kaufmann, *Physica D* **64**, 310 (1993).
- [4] J. M. T. Thompson, *Proc. R. Soc. A* **421**, 195 (1989).
- [5] R. Chacón, F. Balibrea, and M. A. López, *J. Math. Phys.* **37**, 5518 (1996).
- [6] R. Chacón and J. A. Martínez, *Phys. Rev. E* **65**, 036213 (2002).
- [7] H. L. F. Helmholtz, *On the Sensation of Tone as a Physiological Basis for the Theory of Music* (Dover, New York, 1954).
- [8] V. K. Melnikov, *Tr. Mosk. Ova.* **12**, 3 (1963) [Trans. Moscow Math. Soc. **12A**, 1 (1963)].
- [9] J. Guckenheimer and P. J. Holmes, *Nonlinear Oscillations, Dynamical Systems, and Bifurcations of Vector Fields* (Springer, Berlin, 1983).
- [10] F. C. Moon and G.-X. Li, *Phys. Rev. Lett.* **55**, 1439 (1985).
- [11] S. W. McDonald, C. Grebogi, E. Ott, and J. A. Yorke, *Physica D* **17**, 125 (1985).
- [12] For a recent review, see R. Chacón, *Philos. Trans. R. Soc. A* **364**, 2335 (2006).
- [13] I. S. Gradshteyn and I. M. Ryzhik, *Table of Integrals, Series, and Products* (Academic Press, San Diego, 1980).
- [14] J. V. Armitage and W. F. Eberlein, *Elliptic Functions* (Cambridge University Press, Cambridge, England, 2006).
- [15] J. M. T. Thompson, S. R. Bishop, and L. M. Leung, *Phys. Lett. A* **121**, 116 (1987).
- [16] J. M. T. Thompson and M. S. Soliman, *Proc. R. Soc. London, Ser. A* **428**, 1 (1990).
- [17] M. Abramowitz and I. A. Stegun, *Handbook of Mathematical Functions* (Dover, New York, 1972), Chap. 17.
- [18] R. Chacón and A. Martínez García-Hoz, *J. Math. Phys.* **43**, 3586 (2002).
- [19] R. Meucci, W. Gadowski, M. Ciofini, and F. T. Arecchi, *Phys. Rev. E* **49**, R2528 (1994).
- [20] Z. Qu, G. Hu, G. Yang, and G. Qin, *Phys. Rev. Lett.* **74**, 1736 (1995).
- [21] E. del Río, A. Rodríguez Lozano, and M. G. Velarde, *Rev. Sci. Instrum.* **63**, 4208 (1992).